INTERNATIONAL JOURNAL OF STRUCTURAL CHANGES IN SOLIDS – Mechanics and Applications
Volume 3, Number3, 2011, pp.21-34

IJSCS

On the hardening rule for austenitic steels accounting for the strain induced martensitic transformation

G. Ziętek[1*] and Z. Mróz[2]

[1]*Wrocław Technical University, Wrocław, Poland*
[2]*Institute of Fundamental Technological Research, Warsaw, Poland*

Abstract

The elasto-plastic hardening model for austenitic steels undergoing plastic strain induced martensitic transformation is presented with application to both monotonic and cyclic loading processes. The kinematic hardening rule is assumed and expressed in terms of the back stress **Z** composed of two portions **X** and $\mathbf{X}^t$ **,** the first related to plastic strain, the other to phase transformation and volume fraction of martensite. The transformation process is assumed to be driven by the back stress difference **X** – **Y**, where **Y** is the transformation back stress related to growth of the martensitic phase. The non-linear coupling of hardening and phase transformation processes occurs due to interaction of back stresses **X** and $\mathbf{X}^t$. The thermodynamic framework is applied by introducing state variables and conjugate forces used in specifying the plastic flow and evolution rules. The model is applied to simulate cyclic hardening response for uniaxial tension-compression tests and for combined tension-torsion tests. The cyclic stress-strain curves for specified strain amplitudes are used in material parameter calibration.

***Keywords**:* plastic deformation, martensitic transformation, kinematic hardening, back stresses, cyclic deformation, increased hardening rates, decreased ratcheting strains.

Notations

X_{ij}, X_{ij}^t	back stress associated with plastic deformation and martensitic transformation for the yield condition,
Y_{ij}	back stress associated with martensitic transformation for the phase transformation condition,
R_p, R_t, R_l	radius of plastic surface, transformation surface and radius of the limit surface for back stress X_{ij},
ξ, Σ	martensite volume fraction, conjugate generalized force,
$\varepsilon_{ij}^e, \varepsilon_{ij}^p$	elastic strain, plastic strain,
σ_{ij}, s_{ij}	stress, stress deviator,
σ_m, ε_m	hydrostatic stress component, volumetric strain
S	specific entropy per unit mass,
η_{ij}, y_{ij}	microstrains conjugate with X_{ij}, Y_{ij},
$\Psi(\bullet)$,	specific free energy,
$\psi^r(X_{ij})$	recovery potential,
$\dot{\lambda}_1, \dot{\lambda}_2$	Lagrange multipliers.

[*]Corresponding author. E-mail: *grazyna.zietek@pwr.wroc.pl*

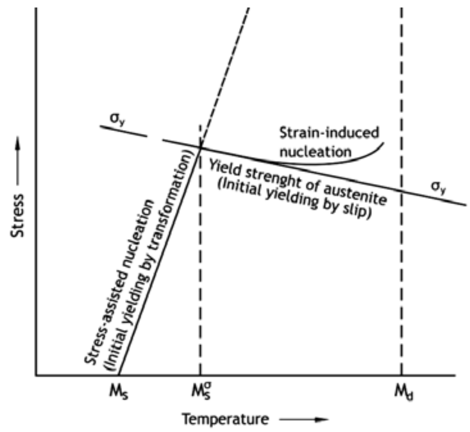

Figure 1. Stress-assisted and strain induced region as function of temperature (Tamura, 1982; Olson and Cohen, 1982)

1. Introduction

Austenitic steels have wide industrial application in view of their physical and mechanical properties, such as corrosion resistance, strength, ductility, weldability, etc. They demonstrate the higher strength/elongation ratios as compared to other metallic structural materials used in automotive or aircraft industry. The microstructural evolution during plastic deformation is related to the low stacking fault energy and strain induced martensitic transformation. This transformation may occur spontaneously in the cooling process below temperature M_s and also induced by stress or plastic strain in metastable austenitic steels at temperatures higher than $T = M_s$, cf. (Abrassart, 1973; Maxwell et al., 1974; Tamura, 1982; Onyuana, 2003; Talonen, 2007).

The martensitic transformation affects essentially mechanical properties of the initial austenitic structure. The nucleation and growth of martensitic phase induce higher plastic hardening rate, both for monotonic and cyclic loading, increases fatigue resistance, but may reduce corrosion resistance (Narutani, 1989; Lebedev and Kosarchuk, 2000; Bracke et al., 2006). Two different martensite phases: paramagnetic hexagonal close-packed (HCP) ε - martensite and ferromagnetic body-centered cubic (BCC) α' - martensite may coexist in the austenitic steels.

The process of mechanically induced martensitic transformation was analyzed by Olson and Cohen (1975, 1982) who assumed two models of nucleation of martensitic plates or needles, namely, stress-assisted martensite and strain-induced martensite. In the first case the applied stress of the value below the yield stress assists or generates the martensitic transformation at the temperature below or above $T = M_s$.The plastic deformation (TRIP) is then caused by the transformation process. In the second case the plastic transformation of austenitic matrix induces nucleation and growth of martensite phase. The spontaneous transformation due to cooling occurs below the temperature M_s. Referring to Figure 1 representing stress-assisted and strain-induced transformation domains in the $\sigma - T$ plane, it is seen that the stress-assisted nucleation occurs below the temperature $T = M_s^\sigma$ when the applied stress reaches the yield stress value σ_Y .Above the temperature $T = M_s^\sigma$ the martensite nucleation occurs due to developed plastic deformation. The temperature $T = M_d$ specifies the end of the transformation process. Different martensitic structures develop depending on the process type cf. (Maxwell et al., 1974; Tamura, 1982; Olson and Azrin, 1982; Das et al., 2008). The martensite form assisted or generated by stress below the yield stress value is the same as that generated by the cooling process, namely in the plate form. The martensite induced by plastic strain has lathlike form. At the temperature near M_s^σ both forms of martensite may coexist. For the temperature increasing above M_s^σ, the needle structures appear at the intersection of shear bands.

The modeling of kinetics of martensitic transformation induced by plastic strain was presented in numerous papers (Olson and Cohen, 1975, 1982; Diani, et al., 1995; Fischer et a.l, 1997; Cherkaoui et al., 1998; Tsuchida and Tomota, 2000). It was assumed that two modes of transformation , namely $\gamma \to \alpha'$, or $\gamma \to \varepsilon \to \alpha'$, where the martensite ε is an intermediate phase. Olson and Cohen (1975) assumed the mode $\gamma \to \alpha'$, but Tjong and Ho (1988) demonstrated that for cyclic deformation the ε - martensite also develops. For the strain amplitude $\varepsilon_a \leq 0.003$ it constitutes the dominating phase and for the strain amplitude increasing to $\varepsilon_a = 0.006$ the lath structure of α' - martensite is generated at the intersection of shear bands, cf. Figure 2.

(a) (b)

Figure 2. Lathlike martensite structure after rupture of tensile specimen: a) steel 321, b) steel 304 (*Fassa et al., 2004; Fassa and Kalete, 2004*).

The experimental works related to the strain induced martensite demonstrated that the martensite phase affects essentially the stress-strain curve. The characteristic inflexion point appears at which the curve slope start to increase in continuing deformation (Perdahcioğlu, et al., 2008; Mughrabi and Christ, 1997). This effect is also observed during cyclic loading (Iwamoto, et al., 1998; Kaleta and Ziętek, 1998; Tomita and Iwamoto, 2001). The effect of strain state that is of tensile and compressive strains on the rate of growth of martensite phase was investigated (Lebedev and Kosarchuk, 2000; Hecker, et al., 1982). The results are not conclusive (Lebedev and Kosarchuk, 2000; Hecker, et al., 1982). In Hecker, et al. (1982) it was concluded that for small strains the rate of growth is higher in the compressive state but for larger strain values the higher growth rate occurs in the tensile state. In cyclic deformation the martensite growth occurs in consecutive cycles when the strain amplitude exceeds the threshold value (Mughrabi and Christ, 1997; Kaleta and Ziętek, 1998; Ganesh, et al., 1994).

The volume fraction of martensite in the austenite matrix is denoted by ξ. For the stress assisted growth the total strain is decomposed into elastic, transformation and plastic parts. For the strain-induced martensite the volume fraction ξ is related to total or plastic strain. Such relation based on uniaxial tensile or compressive tests has been proposed by Angel (1954), next Ludwikson and Berger (1969) in the form

$$\ln\frac{\xi}{1-\xi} = n\ln\varepsilon + k \tag{1}$$

where n and k are the material parameters and ε is the total or plastic strain. However, the most popular is the Olson and Cohen (1975) relation specifying the process kinetics in the form

$$\dot{\xi} = Ap(1-\xi)\dot{\varepsilon}^{slip} \tag{2}$$

where

$$A = \alpha n\eta(\xi^{sb})^{n-1}(1-\xi^{sb}), \tag{3}$$

Here ε^{slip} is the plastic strain associated with crystalline slip, ξ^{sb} denotes the slip band density, p is the probability of martensite incubation at the intersection of slip bands, n and η are the material parameters usually depended on the temperature. The generalization of this relation was proposed by Stringfellow et al. (1992), namely:

$$\dot{\xi} = (1-\xi)(Ap\dot{\varepsilon}^{slip} + B\dot{\tilde{\sigma}}) \tag{4}$$

where $\dot{\tilde{\sigma}}$ is the rate of hydrostatic stress component. The cyclic deformation and martensitic transformation was analyzed by Garion i Skoczeń (2002). The evolution relation of ξ was proposed in the form

$$\dot{\xi} = A(T,\sigma,\dot{\varepsilon}^{p})H((q-q_{\xi})(\xi_L-\xi))\dot{q} \tag{5}$$

Where A is the function of temperature, stress and plastic strain rate, q denotes the accumulated plastic strain and q_{ξ} is the threshold value of q characterizing onset of transformation, H is the Heaviside function and ξ_L is the martensite saturation value. It was also assumed that the yield stress and the hardening modulus depend on the volume fraction ξ.

The martensite transformation is an irreversible process and its evolution is specified in terms of thermodynamic forces associated with the structural transformation. Alternatively, the transformation condition can be expressed in the stress space by introducing the transformation surface similar to the yield surface and the associated flow rule, cf. Fischer *et al.* (1997, 2000). Levitas *et al.* (1998, 1999) presented thermodynamic framework of martensite transformation and specified the dissipation rate. The initiation and growth of martensite has been treated in literature at different scales, micro (Fischer, *et al.*, (1997); Cherkaoui, *et al.*, (1998); Tsuchida and Tomota, 2000), mezo (Levitas *et al.*, 1999) and macroscale, usually applying the homogenization procedure.

The present paper is aimed at formulation of the constitutive model of plastic deformation coupled with the martensite growth during monotonic and cyclic loading. The plastic deformation is specified by the associated flow rule and the yield condition dependent on the stress and the back stress **Z** which is decomposed into the back stress **X** associated with plastic deformation and the back stress $\mathbf{X}^t$ associated with the martensitic transformation $\mathbf{Z}=\mathbf{X}+\mathbf{X}^t$. The constitutive model proposed in the previous paper (Mróz and Ziętek, 2007) is now modified by introducing the transformation surface in the back stress space. In Section 2 the constitutive equations are presented and in Section 3 the model is applied to simulate uniaxial cyclic deformation curves and combined cyclic tension and torsion tests with account for martensite evolution. It is shown that the so called "abnornal hardening" rate induced by phase transformation can be well simulated with characteristic shape of hysteretic loops. In the combined cyclic tension-torsion tests the accumulated ratcheting strain is essentially reduced due to progressing phase transformation.

2. Constitutive model formulation

The constitutive model is based on the assumption of the kinematic hardening rule with neglect of isotropic hardening. This assumption is based on the observation that during cyclic tension-compression tests with accompanying phase transformation the elastic domain (defined by a small offset value) does not expand and can be assumed as fixed. Two irreversible coupled processes proceed in the material that is plastic deformation composed of shear strains on crystallographic slip planes and induced martensitic transformation usually initiating at the intersection of shear bands. The yield condition is assumed in the form

$$F_p = \sqrt{\tfrac{3}{2}(s_{ij} - Z_{ij})(s_{ij} - Z_{ij})} - R_p \le 0, \tag{6}$$

where Z_{ij} is the total back stress which is assumed to be composed of two portions, the first X_{ij} associated with the plastic deformation, the other X_{ij}^t associated with the martensitic transformation, thus

$$Z_{ij} = X_{ij} + X_{ij}^t. \tag{7}$$

The phase transformation condition is assumed in the form

$$F_{tr} = \sqrt{\tfrac{3}{2}(X_{ij} - Y_{ij})(X_{ij} - Y_{ij})} - R_t(\Sigma,\sigma_m) \le 0 \tag{8}$$

and is expressed in terms of the back stress X_{ij} reaching the critical value dependent on the generalized force Σ conjugate to the martensite volume fraction ξ and the hydrostatic stress component $\sigma_m = \frac{1}{3}\sigma_{kk}$. The back stress Y_{ij} growing during the phase transformation specifies the translation of the surface $F_{tr}=0$ in the back stress space. Following the previous paper (Mróz and Ziętek, 2007) it is assumed that

$$X_{ij}^t = a(\xi)\left(\sqrt{\tfrac{3}{2}Y_{kl}Y_{kl}}\right)^n Y_{ij} = a(\xi)(Y_e)^n Y_{ij}, \quad Y_e = \left(\tfrac{3}{2}Y_{kl}Y_{kl}\right)^{1/2} \tag{9}$$

where $a(\xi)$ is the monotonically increasing and bounded function of ξ, thus $a(0)=0$ and $a(\xi) \to a^*$ for $\xi \to \xi^*$ where a^* and ξ^* are the saturation values. The effect of the back stress **Y** increases with the growth of the martensitic phase. For n=2 and $R_t = 0$ there is **X=Y** and the model formulation of the previous paper (Mróz and Ziętek, 2007) is obtained.

The elastic state of material is specified in terms of state parameters and conjugate forces, thus

$$\boldsymbol{\alpha}_1 = (\boldsymbol{\varepsilon}^e, T) \rightarrow \mathbf{A}_1 = (\boldsymbol{\sigma}, S) \tag{10}$$

where $\boldsymbol{\varepsilon}^e = [\varepsilon_{ij}^e]$ is the elastic strain, T denotes temperature, $\boldsymbol{\sigma} = [\sigma_{ij}]$ is the stress tensor and S is the specific entropy per unit mass. The inelastic response is expressed in terms of the internal state variables and conjugate forces, namely

$$\boldsymbol{\alpha}_2 = (\boldsymbol{\eta}, \mathbf{y}, \xi,) \rightarrow \mathbf{A}_2 = (\mathbf{X}, \mathbf{Y}, \Sigma) \tag{11}$$

where $\boldsymbol{\eta} = [\eta_{ij}]$ and $\mathbf{y} = [y_{ij}]$ are the microstrains conjugate with the forces **X** and **Y**. The specific free energy for the isothermal process is assumed in the form

$$\rho\tilde{\Psi} = \Psi(\boldsymbol{\alpha}_1, \boldsymbol{\alpha}_2) = \tfrac{1}{2}L_{ijkl}\varepsilon_{ij}^e\varepsilon_{kl}^e + \tfrac{1}{3}C_1\eta_{ij}\eta_{ij} + \tfrac{1}{3}C_2 y_{ij}y_{ij} + \varphi(\xi) \tag{12}$$

For simplicity, the elastic moduli of austenite and martensite are assumed to be the same , with the elasticity matrix L_{ijkl}. The elastic moduli for microstrain energy terms are C_1 and C_2.

The specific dissipation rate follows from the second law of thermodynamics

$$\dot{D} = \sigma_{ij} \cdot \dot{\varepsilon}_{ij} - \rho \dot{\Psi} \geq 0 \tag{13}$$

Decompose the total strain rate into elastic, plastic and transformation components: $\dot{\varepsilon}_{ij} = \dot{\varepsilon}_{ij}{}^{e} + \dot{\varepsilon}_{ij}{}^{p} + \dot{\varepsilon}_{ij}{}^{t}$. In view of (13), the forces conjugate to elastic and inelastic state variables are

$$\begin{aligned} \sigma_{ij} &= \frac{\partial \Psi}{\partial \varepsilon_{ij}^{e}} = L_{ijkl}\varepsilon_{kl}^{e}, \qquad X_{ij} = \frac{\partial \Psi}{\partial \eta_{ij}} = \tfrac{2}{3} C_1 \eta_{ij}, \\ Y_{ij} &= \frac{\partial \Psi}{\partial y_{ij}} = \tfrac{2}{3} C_2 y_{ij}, \qquad \Sigma = \frac{\partial \Psi}{\partial \xi} = \frac{d\varphi}{d\xi}. \end{aligned} \tag{14}$$

And

$$\dot{D} = \sigma_{ij} \cdot (\dot{\varepsilon}_{ij}{}^{p} + \dot{\varepsilon}_{ij}{}^{t}) - X_{ij} \cdot \dot{\eta}_{ij} - Y_{ij} \cdot \dot{y}_{ij} - \Sigma \cdot \dot{\xi} \geq 0 \tag{15}$$

The back stress **X** can be regarded as the local fluctuation (self equilibrated residual stress) induced by the inhomogeneous plastic deformation within the crystalline grain. Similarly, **Y** is the fluctuation stress induced by the martensitic transformation. The transformation process is assumed to start when the effective scalar back stress reaches a critical value and proceeds with the accompanied growth of the transformation back stress **Y.** The deviatoric component of the transformation strain is neglected, only volumetric strain is specified, thus $\varepsilon_{ij}{}^{t} = \varepsilon_m \delta_{ij}$.

The microstrains η_{ij} and y_{ij} are the conjugate variables used to specify the free energy terms of (14). They represent strain fluctuations in the representative element, not affecting the macro-strain $\boldsymbol{\varepsilon}$, only inducing coupled hardening effect. These microstrains do not occur in the finite form of constitutive relations.
Two major cases now occur, namely, the plastic flow with no phase transformation and the plastic flow coupled with martensite evolution.

2.1. Plastic flow

Now, we have

$$F_p = 0, \quad \dot{F}_p = 0, \quad F_{tr} < 0 \text{ or } F_{tr} = 0, \ \dot{F}_{tr} < 0 \tag{16}$$

and the plastic deformation of the austenite occurs. Assume the associated flow rule

$$\dot{\varepsilon}_{ij}^{p} = \dot{\lambda}_1 \frac{\partial F_p}{\partial \sigma_{ij}} = \dot{\lambda}_1 N_{ij} = \dot{\lambda}_1 \frac{3(s_{ij} - X_{ij})}{2R_p} \tag{17}$$

and the microstrain rate $\dot{\eta}_{ij}$ governed by the yield condition and the recovery potential $\psi^r = \psi^r(\mathbf{X})$, thus

$$\dot{\eta}_{ij} = -\dot{\lambda}_1 \left(\frac{\partial F_p}{\partial X_{ij}} + \frac{\partial \psi^r}{\partial X_{ij}} \right), \quad \psi^r = \frac{1}{2} C X_{ij} X_{ij}, \tag{18}$$

and

$$\dot{X}_{ij} = \tfrac{2}{3} C_1 \dot{\eta}_{ij} = \tfrac{2}{3} C_1 (N_{ij} - C X_{ij}) \dot{\lambda}_1 = \tfrac{2}{3} C_1 \dot{\lambda}_1 (X_{ij}^{(l)} - X_{ij}), \tag{19}$$

where the plastic multiplier equals $\dot{\lambda}_1 = \sqrt{\frac{2}{3} \dot{\varepsilon}_{ij}^{p} \dot{\varepsilon}_{ij}^{p}}$ and $\mathbf{X}^{(l)}$ is the back stress on the limit surface

$$F_l(\mathbf{X}) = \sqrt{\tfrac{3}{2} X_{ij} X_{ij}} - \frac{3}{2C} = \sqrt{\tfrac{3}{2} X_{ij} X_{ij}} - R_l = 0, \tag{20}$$

And $R_l = \dfrac{3}{2C}$ is the radius of the limit surface for the back stress **X**, cf. (Mróz and Ziętek, 2007). The back stress evolution rule follows the Frederick-Armstrong rule used frequently in the cyclic plasticity models (Frederick and Armstrong, 2007). The hardening modulus H is specified from the consistency condition

$$\frac{\partial F_p}{\partial \sigma_{ij}} \dot{\sigma}_{ij} = \dot{\lambda}_1 H \tag{21}$$

and there is

$$H = \tfrac{2}{3} C_1 \left(X_{ij}^{(l)} - X_{ij} \right) N_{ij}. \tag{22}$$

When the martensitic transformation occurred in the previous stage with subsequent unloading on transformation surface the flow rule has the form

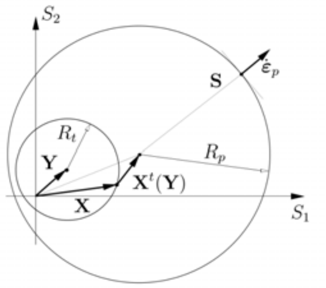

Figure 3. The yield and transformation surfaces $F_p = 0$, $F_{tr} = 0$ in the stress space.

$$\dot{\varepsilon}_{ij}^{p} = \dot{\lambda}_1 N_{ij} = \dot{\lambda}_1 \frac{3(s_{ij} - X_{ij} - X_{ij}^{t})}{2R_p} \tag{23}$$

and

$$F_{tr} < 0 \ \text{ or } \ F_{tr} = 0 \ \text{ i } \ \frac{\partial F_{tr}}{\partial X_{ij}} \dot{X}_{ij} < 0 \tag{24}$$

The martensitic phase does not grow but the transformation surface as the result of plastic deformation translates in accordance with the evolution equation

$$\dot{y}_{ij} = -\dot{\lambda}_1 \frac{\partial F_p}{\partial Y_{ij}} = \dot{\varepsilon}_{kl}^{p} \frac{\partial X_{kl}^{t}}{\partial Y_{ij}} \,. \tag{25}$$

2.2. *Coupled plastic deformation and phase transformation.*

The coupled plastic deformation and phase transformation processes occur when

$$F_p = 0, \quad \dot{F}_p = 0, \quad F_{tr} = 0, \quad \dot{F}_{tr} = 0 \tag{26}$$

Similarly as in the previous case, the plastic flow rule has the form

$$\dot{\varepsilon}_{ij}^{p} = \dot{\lambda}_1 \frac{\partial F_p}{\partial \sigma_{ij}} + \dot{\lambda}_2 \frac{\partial F_{tr}}{\partial \sigma_{ij}} = \dot{\lambda}_1 \frac{3(s_{ij} - X_{ij} - X_{ij}^{t}(\mathbf{Y}))}{2R_p} - \dot{\lambda}_2 \frac{\partial R_t}{\partial \sigma_{ij}} \tag{27}$$

The deformation strain rate has now the volumetric term specified by the relation

$$\dot{\varepsilon}_m = -\tfrac{1}{3} \dot{\lambda}_2 \frac{\partial R_t}{\partial \sigma_m} \,. \tag{28}$$

The radius of the transformation surface should be a decreasing function of the hydrostatic stress σ_m. Let us note that both plastic and transformation strain rates are included in one term (27). The evolution rules of the microstrains y_{ij} and η_{ij} are

$$\dot{y}_{ij} = -\dot{\lambda}_1 \frac{\partial F_p}{\partial Y_{ij}} - \dot{\lambda}_2 \frac{\partial F_{tr}}{\partial Y_{ij}} = \dot{\lambda}_1 \frac{\partial F_p}{\partial \sigma_{kl}} \frac{\partial X_{kl}^{t}}{\partial Y_{ij}} + \dot{\lambda}_2 \frac{\partial F_{tr}}{\partial X_{ij}} = \left(\dot{\varepsilon}_{kl}^{p} - \dot{\varepsilon}_m \delta_{kl}\right) \frac{\partial f_{kl}}{\partial Y_{ij}} + \dot{\lambda}_2 \frac{3(X_{ij} - Y_{ij})}{2R_t} \tag{29}$$

and

$$\dot{\eta}_{ij} = -\dot{\lambda}_1 \left(\frac{\partial F_p}{\partial X_{ij}} + \frac{\partial \psi^r}{\partial X_{ij}} \right) - \dot{\lambda}_2 \frac{\partial F_{tr}}{\partial X_{ij}} = \left(\dot{\varepsilon}_{ij}^{p} - \dot{\varepsilon}_m \delta_{ij}\right) - C X_{ij} \dot{\lambda}_1 - \dot{\lambda}_2 \frac{3(X_{ij} - Y_{ij})}{2R_t} \tag{30}$$

The multipliers $\dot{\lambda}_1$ and $\dot{\lambda}_2$ are expressed from the consistency conditions

$$\dot{\lambda}_1 = \frac{1}{H_1} \frac{\partial F_p}{\partial \sigma_{ij}} \dot{\sigma}_{ij} \,, \ \dot{\lambda}_2 = \frac{1}{H_2} \frac{\partial F_p}{\partial \sigma_{ij}} \dot{\sigma}_{ij} \tag{31}$$

and the detailed derivation is presented in Appendix. The martensite evolution rule can be derived from the transformation condition (8), thus

$$\dot{\xi} = -\dot{\lambda}_2 \frac{\partial F_{tr}}{\partial \Sigma} = \dot{\lambda}_2 \frac{dR_t}{d\Sigma} \tag{32}$$

The relative configuration of yield and transformation surfaces is presented in Figure 3.

2.3.Selection of material functions

The back stress function $\mathbf{X}^t(\mathbf{Y},\xi)$ is specified by (9). In this paper it is assumed that n=1 and we have

$$X_{ij}^t(\mathbf{Y},\xi) = a(\xi)\left(\sqrt{\tfrac{3}{2}\tilde{Y}_{kl}\tilde{Y}_{kl}}\right)Y_{ij} = a(\xi)\tilde{Y}_e Y_{ij} \tag{33}$$

where

$$\widetilde{Y}_{kl} = \frac{Y_{kl}}{\sigma_r}, \quad \widetilde{Y}_e = \frac{Y_e}{\sigma_r} \tag{34}$$

and σ_r is the reference stress to render $\widetilde{Y}_{kl}$ and $\widetilde{Y}_e$ non-dimensional. The free energy function associated with transformation, the conjugate force Σ and the radius of the transformation surface are

$$\varphi(\xi) = \tfrac{1}{2}b\xi^2, \quad \Sigma = \frac{d\varphi}{d\xi} = b\xi, \quad R_t = R_{st} - \tfrac{1}{2}h(\sigma_m)(b-\Sigma)^2 = R_{st} - \tfrac{1}{2}bh(\sigma_m)(1-\xi)^2 \tag{35}$$

where R_{st} is the saturation value of R_t. The stress function $h(\sigma_m)$ should be monotonically growing with σ_m, so it is assumed in the non-dimensional form

$$h(\sigma_m) = h(\widetilde{\sigma}_m) = e^{k\widetilde{\sigma}_m}, \quad \widetilde{\sigma}_m = \frac{\sigma_m}{\sigma_r} \tag{36}$$

The martensite evolution rule is obtained from (32) as

$$\dot{\xi} = \dot{\lambda}_2 h(\widetilde{\sigma}_m)(b-\Sigma) = \dot{\lambda}_2 bh(\widetilde{\sigma}_m)(1-\xi) \tag{37}$$

and the volumetric transformation strain equals

$$\dot{\varepsilon}_m = \tfrac{1}{6}\dot{\lambda}_2(b-\Sigma)^2\frac{1}{\sigma_r}\frac{dh}{d\widetilde{\sigma}_m} = \tfrac{1}{6}\dot{\lambda}_2 b^2(1-\xi)^2\frac{kh(\widetilde{\sigma}_m)}{\sigma_r} \tag{38}$$

Integrating relation (37), one obtains

$$\xi = 1 - e^{-b\int_0^{\lambda_2} h(\widetilde{\sigma}_m)d\lambda_2}. \tag{39}$$

The rate of evolution of ξ now depends on the sign of mean hydrostatic stress, thus predicting different rate in tension and compression tests.

3. Model application to simulation of uniaxial and biaxial cyclic deformation

3.1. Cyclic deformation for uniaxial tension – compression loading.

Consider first the uniaxial deformation in cyclic tension – compression loading program. The yield condition (6) now has the form

$$F_p = \left|\sigma - X - a(\xi)\frac{Y^2}{\sigma_r}signY\right| - R_p \le 0 \tag{40}$$

and the transformation condition is expressed as follows

$$F_{tr} = |X - Y| - R_t(\Sigma,\sigma) \le 0\,. \tag{41}$$

The relation (14) between the state variables and the conjugate forces are

$$X = C_1\eta, \quad Y = C_2 y, \quad \Sigma = \frac{d\varphi}{d\xi} = \varphi'(\xi). \tag{42}$$

When only the plastic deformation occurs, then $F_p = 0$, $F_{tr} < 0$, and from (17) it follows that

$$\dot{X} = C_1\left[\dot{\varepsilon}_p - \tfrac{2}{3}CX\left|\dot{\varepsilon}_p\right|\right] \tag{43}$$

and

$$\dot{Y} = 2a(\xi)|Y|\dot{\varepsilon}_p\,. \tag{44}$$

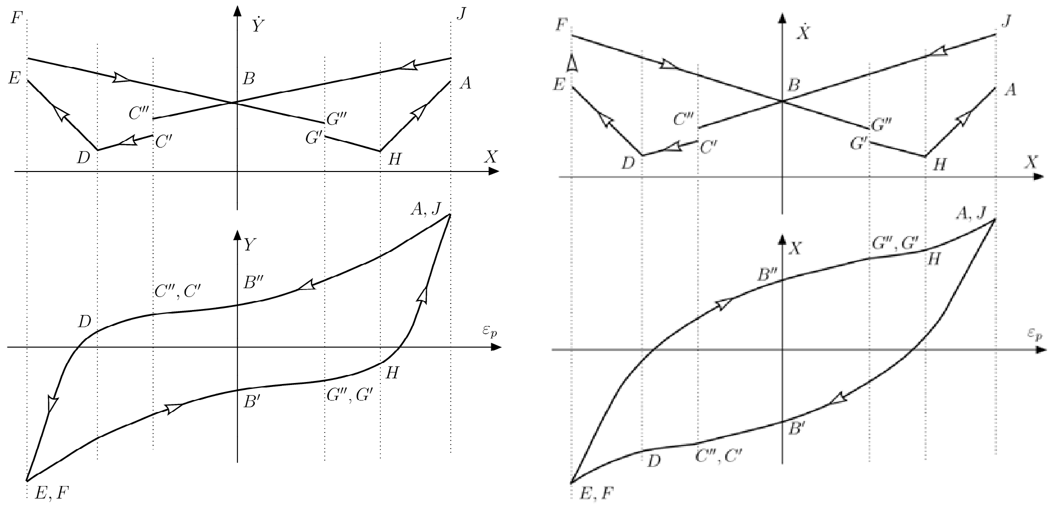

(a) (b)

Figure 4. Evolution of the back stresses X and Y during one cycle.

When both plastic deformation and phase transformation takes place, from (14), (29) and (30) the following evolution relation results

$$\begin{aligned}
&\dot{X} = C_1\left[\left(1+2a(\xi)\left|X \mp R_t\right|\right)(\dot{\varepsilon}_p - \dot{\varepsilon}_m) - \frac{\dot{Y}}{C_2} - \tfrac{2}{3}CX\left|\dot{\varepsilon}_p - \dot{\varepsilon}_m\right|\right],\\
&\dot{\xi} = \dot{\lambda}_2 b h(\widetilde{\sigma})(1-\xi),\\
&\dot{Y} = \dot{X} \pm \left(\frac{\partial R_t}{\partial \Sigma}\dot{\Sigma} + \frac{1}{\sigma_r}\frac{\partial R_t}{\partial \widetilde{\sigma}}\dot{\sigma}\right) = \dot{X} \pm b\left(h(\widetilde{\sigma})(1-\xi)\dot{\xi} - \frac{1}{2\sigma_r}\frac{dh(\widetilde{\sigma})}{d\widetilde{\sigma}}(1-\xi)^2\dot{\sigma}\right).
\end{aligned} \tag{45}$$

For states close to the saturation of phase transformation, from (45) it follows that

$$\dot{X} = \frac{C_1 C_2}{C_2 + C_1}\left[(1 + 2a^*\left|X \pm R_t\right|)\dot{\varepsilon}_p - \tfrac{2}{3}CX\left|\dot{\varepsilon}_p\right|\right] \tag{46}$$

where $a^* = a(\xi^*)$.

Consider now the process of uniaxial cyclic tension – compression of specified plastic strain amplitude ε_{ap}. For the reloading from the reversal state, the evolution of back stress X is obtained by integrating (43), thus

$$X(\varepsilon_p) = \left(-X_a - \frac{3}{2C}\right)\mathrm{e}^{-\frac{2}{3}CC_1(\varepsilon_p + \varepsilon_{ap})} + \frac{3}{2C} \tag{47}$$

The transformation surface becomes active when $X(\varepsilon_p) = -X_a + 2R_t$ and from (45) and (47) we obtain

$$X(\varepsilon_p) = \begin{cases} \left(-X_a + 2R_t - B_2\right)e^{-B_1(\varepsilon_p - \varepsilon_{p1})} + B_2 & \text{dla} \quad X < R_t \\ \left(R_t - B_2\right)e^{B_3(\varepsilon_p - \varepsilon_{p2})} + B_4 & \text{dla} \quad X \geq R_t \end{cases} \tag{48}$$

Where

$$\begin{aligned}
&B_1 = \frac{C_1 C_2}{C_1 + C_2}\left(\tfrac{2}{3}C + 2a^*\right), \quad B_2 = \frac{C_1 C_2}{C_1 + C_2}\frac{1 + 2a^* R_t}{\left(\tfrac{2}{3}C + 2a^*\right)},\\
&B_3 = \frac{C_1 C_2}{C_1 + C_2}\left(2a^* - \tfrac{2}{3}C\right), \quad B_4 = \frac{C_1 C_2}{C_1 + C_2}\frac{1 - 2a^* R_t}{\left(2a^* - \tfrac{2}{3}C\right)}, \quad X(\varepsilon_{p2}) = R_t.
\end{aligned} \tag{49}$$

The evolution of the back stresses X and Y during one cycle is shown in Figure 4.

3.2 Biaxial stress state: combined torsion and tension.

The shear stress $\tau_{12} = \tau_{21} = \tau$ and longitudinal stress $\sigma_{11} = \sigma$ are applied in the case of combined tension and torsion. The yield condition (6) has now the form

$$F_p = \sqrt{\left[\sigma - X_\sigma - a(\xi)Y_\sigma \tilde{Y}_e\right]^2 + 3\left[\tau - X_\tau - a(\xi)Y_\tau \tilde{Y}_e\right]^2} - R_p \le 0, \quad \tilde{Y}_e = \sqrt{\tilde{Y}_\sigma^2 + 3\tilde{Y}_\tau^2} \tag{50}$$

and the transformation condition may be expressed by

$$F_{tr} = \sqrt{(X_\sigma - Y_\sigma)^2 + 3(X_\tau - Y_\tau)^2} - R_t \le 0 \tag{51}$$

The relations (14) between the state variables and the conjugate forces are

$$\begin{aligned} X_\sigma &= C_1\eta_{11}, \quad Y_\sigma = C_2 y_{11}, \\ X_\tau &= \tfrac{2}{3}C_1\eta_{12}, \quad Y_\tau = \tfrac{2}{3}C_2 y_{12}, \end{aligned} \quad \Sigma = \varphi'(\xi). \tag{52}$$

The evolution of shear and axial strains may be obtained by applying the associated flow rule (17)

$$\dot{\varepsilon}_{11}^p = \dot{\lambda}_1 \frac{\sigma - X_\sigma - a(\xi)\tilde{Y}_e Y_\sigma}{R_p} + \frac{1}{6}\frac{b^2}{\sigma_r}(1-\xi)^2 \frac{dh}{d\tilde{\sigma}}\dot{\lambda}_2, \quad \dot{\varepsilon}_{12}^p = \dot{\lambda}_1 \frac{3(\tau - X_\tau - a(\xi)\tilde{Y}_e Y_\tau)}{2R_p} \tag{53}$$

where

$$\dot{\lambda}_1 = \sqrt{\left(\dot{\varepsilon}_{11}^p - \dot{\varepsilon}_m\right)^2 + \tfrac{4}{3}\left(\dot{\varepsilon}_{12}^p\right)^2} \tag{54}$$

Similarly as in the uniaxial state, when only plastic deformation occurs ($F_p = 0,\ \dot{F}_p = 0$ and $F_{tr} < 0$), the evolution equations for the back stress take the form

$$\begin{aligned} \dot{\eta}_{11} &= \dot{\varepsilon}_{11}^p - CX_\sigma \dot{\lambda}_1 \quad \Rightarrow \quad \frac{\dot{X}_\sigma}{C_1} = \dot{\varepsilon}_{11}^p - \tfrac{2}{3}CX_\sigma\dot{\lambda}_1 \\ \dot{\eta}_{12} &= \dot{\varepsilon}_{12}^p - CX_\tau \dot{\lambda}_1 \quad \Rightarrow \quad \frac{\dot{X}_\tau}{\frac{2}{3}C_1} = \dot{\varepsilon}_{12}^p - CX_\tau\dot{\lambda}_1 \end{aligned} . \tag{55}$$

The evolution of the center of the transformation surface is specified by the relations:

$$\begin{aligned} \dot{Y}_\sigma &= C_2 \dot{y}_{11} \\ \dot{Y}_\tau &= \frac{2}{3}C_2 \dot{y}_{12} \end{aligned} \tag{56}$$

The additional terms occur in equations (55) and (56) when the martensitic transformation takes place. The evolution rules for transformation of back stress then take the form

$$\begin{aligned} \frac{\dot{Y}_\sigma}{C_2} &= -\dot{\lambda}_1\frac{\partial F_p}{\partial Y_\sigma} - \dot{\lambda}_2\frac{\partial F_{tr}}{\partial Y_\sigma} \quad \Rightarrow \quad \dot{\lambda}_2\frac{(X_\sigma - Y_\sigma)}{R_t} = \frac{\dot{Y}_\sigma}{C_2} - a(\xi)\left[\left(\frac{Y_\sigma^2}{Y_e} + Y_e\right)(\dot{\varepsilon}_{11}^p - \dot{\varepsilon}_m) + \frac{2Y_\sigma Y_\tau}{Y_e}\dot{\varepsilon}_{12}^p\right], \\ \frac{\dot{Y}_\tau}{\frac{2}{3}C_2} &= -\dot{\lambda}_1\frac{\partial F_p}{\partial Y_\tau} - \dot{\lambda}_2\frac{\partial F_{tr}}{\partial Y_\tau} \quad \Rightarrow \quad \dot{\lambda}_2\frac{3(X_\tau - Y_\tau)}{2R_t} = \frac{\dot{Y}_\tau}{\frac{2}{3}C_2} - a(\xi)\left[\frac{Y_\sigma Y_\tau}{Y_e}(\dot{\varepsilon}_{11}^p - \dot{\varepsilon}_m) + 2\left(\frac{Y_\sigma^2}{Y_e} + Y_e\right)\dot{\varepsilon}_{12}^p\right]. \end{aligned} \tag{57}$$

Taking into account equations (57), the evolution formulae of back stress may be expressed as follows

$$\begin{aligned} \frac{\dot{X}_\sigma}{C_1} &= (\dot{\varepsilon}_{11}^p - \dot{\varepsilon}_m) - \tfrac{2}{3}CX_\sigma\dot{\lambda}_1 - \dot{\lambda}_2\frac{(X_\sigma - Y_\sigma)}{R_t}, \\ \frac{\dot{X}_\tau}{\frac{2}{3}C_1} &= \dot{\varepsilon}_{12}^p - CX_\tau\dot{\lambda}_1 - \dot{\lambda}_2\frac{2(X_\tau - Y_\tau)}{3R_t}. \end{aligned} \tag{58}$$

The evolution equation for volume fraction of martensite ξ is the same as for the uniaxial case.

4. Identification of parameters of hardening model and its application.

4.1 Parameter specification

The identification procedure has been carried out by using the experimental results presented in Kaleta and Ziętek (1998) and program package for non-linear approximation SigmaPlot®4.0. This program package fits the equations to experimental data using standard curvilinear approximation techniques –least squares minimization of the function and generates full statistical report.

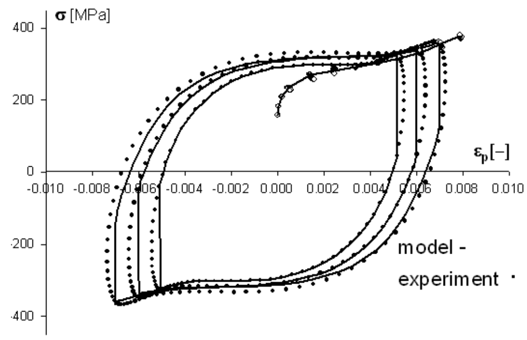

Figure 5. The hysteresis loops derived from model and experiment for different plastic strain amplitudes in the steady state of the cyclic deformation process.

Cylindrical specimens made of austenitic steel 304L were tested under uniaxial tension-compression. The amplitude of plastic strain was controlled during the test. The model parameters were found for the steady state of cyclic deformation. It may be assumed that the volume fraction of martensite is close to its asymptotic value $\xi = \xi^*$ after some number cycles.

The parameters B_1, B_2, B_3 and B_4 were obtained from the identification procedure based on equations (49). This approximation allow us obtain quotient $C_1C_2/(C_1+C_2)$ only, so having value of parameter C parameter C_1 may be found using equation (47) for inactive transformation surface. The following parameter values were specified: $C_1 = 125000\,MPa$, $C_2 = 85000\,MPa$, $C = 0.005$, $a^* = 0.007$ and $R_{st} = 190\,MPa$. Three exemplary loops are presented in Figure 5.

Numerical simulation has been performed for two loading programs: under the conditions of increasing and constant plastic amplitude. For lack of experimental data connected with the growth of martensite, the values of the parameters in the equations (35) – (39) were accepted on the ground literature data (Mahnken, *et al.*, 2009): k=0.01, b=0.1.

*4.2 Simulation of cyclic hysteresis loops during growth of martensitic ph*ase: *uniaxial cyclic loading.*

The simulation was performed for uniaxial cyclic tension – compression at constant plastic strain amplitude as well as at constant stress amplitude. The values of the parameters C_1, C_2 and C were accepted from the identification of hysteresis loops at the steady state. The function $a(\xi)$ was assumed as linear but ξ and R_t were specified by the equations (35) and (39). Results of simulation at constant plastic strain amplitude and constant stress amplitude are presented in Figures 6 and 7.

The obtained results are stable as the small changes of parameters do not cause large changes of the values of stress or the back stress. It is seen that due to transformation induced hardening the transient cyclic deformation proceeds for shrinking stress-strain loops and increasing stress amplitude.

4.3 Cyclic tension – torsion tests of tubular specimens.

The simulation was performed for uniaxial cyclic tension – compression at constant stress amplitude under fixed shear stress value.

The dependence of axial stress and back stress on plastic strain is presented in Figure 8 and the dependence of back stress Y_σ and Y_τ on plastic is demonstrated in Figure 9.

The accumulation of shear strain ε_{12}^p due to cyclically varying axial strain ε_{11}^p is depicted in Figure 10. The growth of martensitic phase causes increase of back stress Y_τ (Figure 9b). For that reason the accumulation of shear strain ε_{12}^p decreases in consecutive cycles. All parameters: axial strain amplitude ε_{a11}^p, accumulated shear strain ε_{12}^p in cyclic deformation , back stress components X_σ, X_τ, Y_σ and Y_τ become stabilized with convergence of the martensite volume fraction ξ to its limit value. Unfortunately, the experimental data related to ratchetting effect combined with martensitic transformation are not available.

The evolution of yield and transformation surfaces during cyclic loading is illustrated in Figure 11.

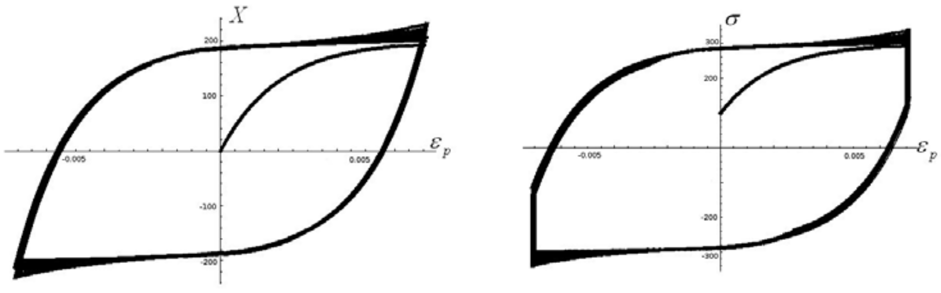

(a) (b)

Figure 6. The evolution of cyclic hysteresis loops for constant plastic strain amplitude: a) back stress - plastic strain, b) stress - plastic strain.

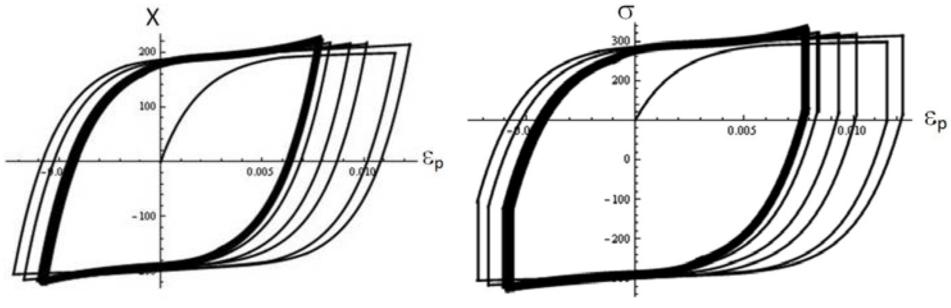

(a) (b)

Figure 7. The evolution of cyclic hysteresis loops for constant stress amplitude: a) back stress - plastic strain, b) stress - plastic strain.

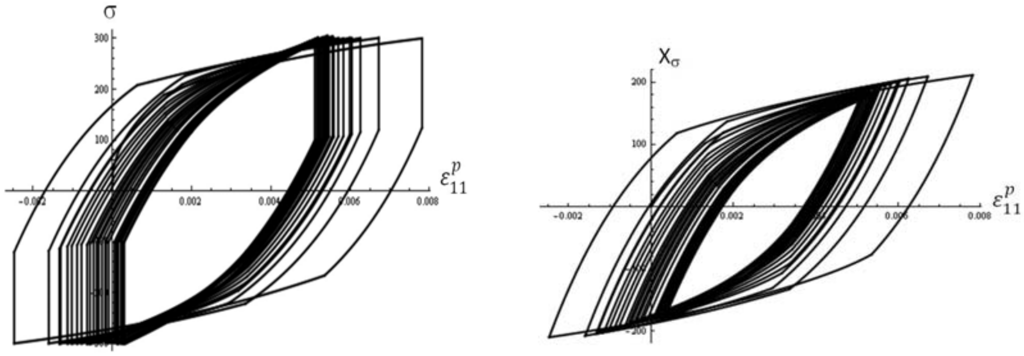

(a) (b)

Figure 8. The evolution of cyclic hysteresis loops for constant axial stress amplitude superposed on fixed shear stress $\tau = 100\, MPa$: a) axial stress - longitudinal plastic strain deviator, b) back stress - axial plastic strain deviator.

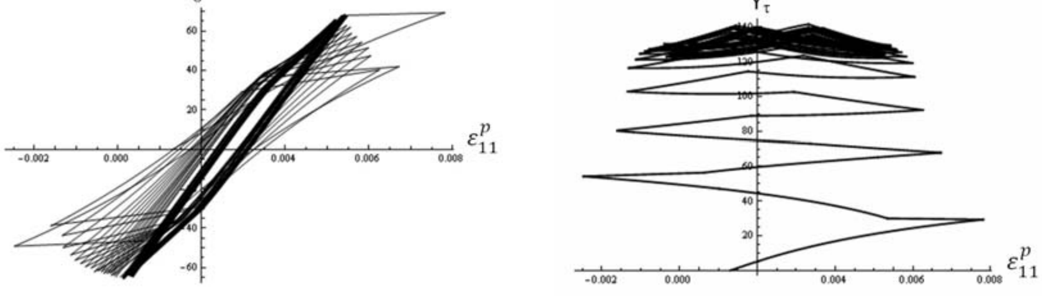

(a) (b)

Figure 9. The evolution of back stress components Y_σ and Y_τ for cyclic constant axial stress amplitude superposed on fixed shear stress $\tau = 100\, MPa$: a) back stress Y_σ - axial plastic strain, b) back stress Y_τ - axial plastic strain.

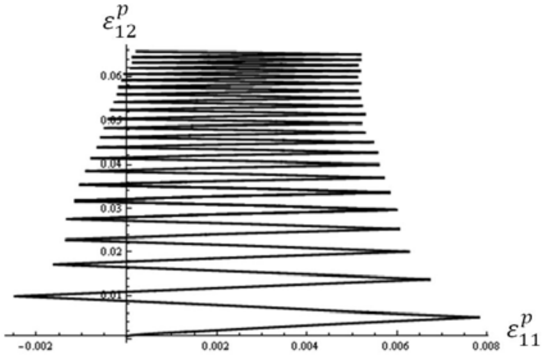

Figure 10. Dependence of the shear strain ε_{12}^{p} on the axial strain ε_{11}^{p} for cyclic tension – compression of specified stress amplitude superposed on fixed shear stress. It is seen that the ratcheting effect disappears due to transformation hardening.

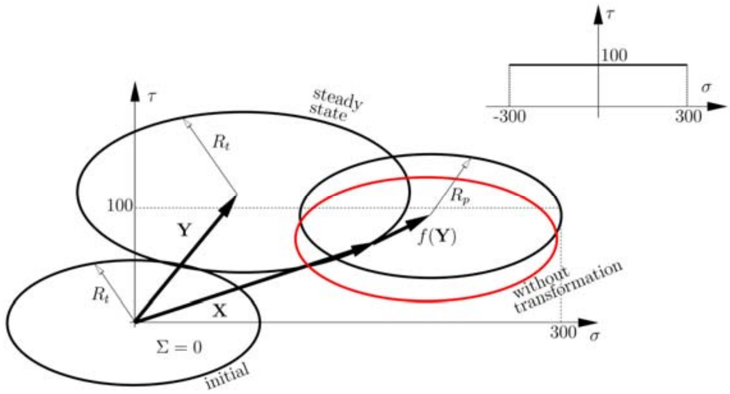

Figure 11. Schematic presentation of the yield and transformation surfaces in the initial and steady states.

5. Concluding remarks

The paper presents the formulation of an of elasto-plastic model for austenitic steels with account for martensitic transformation induced by plastic deformation. Constitutive equations were formulated using the irreversible thermodynamics framework with internal variables. Two irreversible coupled processes proceeding in the material were accounted for by considering plastic deformation and induced martensitic transformation above the transition temperature M_s. The phase transformation condition is expressed in terms of the back stress **X** reaching its critical value dependent on the generalized force conjugate to volume fraction of martensite and the hydrostatic stress. The condition of plastic deformation was assumed in the form of the modified yield surface. This modification allows for the description of evolution of enhanced hardening rate observed for such type of austenitic steel.

It was assumed that the radius of transformation surface depends on the mean stress and generalized transformation force. This relation generates the volumetric strain component and the martensite fraction. Based on experimental data obtained for the steady cyclic deformation, the plastic hardening parameter can be specified. The parameter related to martensitic transformation may be determined from microscopic experiments. However, the presented model requires macroscopic values. The relations specifying the volume fraction of martensite and the respective parameters were fitted by numerical simulations.

References

Abrassart, F., 1973 Stress-induced $\gamma \rightarrow \alpha'$ martensitic transformation in two carbon stainless steels. Application to TRIP steels, Metallurgical Transaction, 4, 2205 – 2216.

Angel, T., 1954 Formation of martensite in austenitic stainless steels. Effects of deformation, temperature, and composition, Journal of the Iron and Steel Institute, 177, 165 – 174.

Bracke, L., Mertens, G., Penning, J., de Cooman, B. C., Liebeherr, M., and Akdut, N., 2006 Influence of phase transformations on the mechanical properties of high-strength austenitic Fe-Mn-Cr steel, Metallurgical and Materials Transaction A, 37A, 307 – 317.

Cherkaoui, M., Berveiller, M., and Sabar, H., 1998 Micromechanical modelling of martensitic transformation induced plasticity (TRIP) in austenitic single crystals, International Journal of Plasticity, 14, 597 – 626.

Das, A., Sivaprasad, S., Ghosh, M., Chakraborti, P. C., and Tarafder, S., 2008 Morphologies and characteristics of deformation induced martensite during tensile deformation of 304 LN stainless steel, Materials Science & Engineering A, 486, 283 – 286.

Diani, J. M.,Sabar, H., and Berveiller, M., 1995 Micromechanical modelling of the transformation induced plasticity (TRIP) phenomenon in steels, International Journal Engineering Science, 33, 1921 – 1934.

Fassa, B., Kaleta, J., and Wiśniewski W., 2004 Investigation of kinetics of athermal martensitic transformation induced by cyclic deformation of austenite, in Proceedings 21^{st} Symposium on Experimental Mechanics of Solids, Jachranka, 201 – 206, (in Polish).

Fassa, B., Kaleta, J., Smaga, M., and Wiśniewski, W., 2004 Magnetic metod of investigation of kinetics of athermal martensitic transformation induced by cyclic deformation of austenite, in Proceedings of XX Symposium “Fatigue and Fracture Mechanics”, Bydgoszcz, 57 – 63, (in Polish).

Fischer, F. D., Antretter, T., Azzouz, F., Cailletaud, G., Pineau A., Tanaka, K. and Nagayama, K., 2000 The role of backstress in phase transforming steels, Arch. Mech., 52, 569 – 588.

Fischer, F. D., Oberaigner, E. R., and Tanaka, K., 1997 A micromechanical approach to constitutive equations for phase changing materials, Computational Materials Science, 9, 56 – 63.

Frederick, C. O., and Armstrong, P. J., 2007 A mathematical representacjon of multiaxial Bauschinger effect, Materials at High Temperature, 24(1), 1 -26.

Ganesh Sundara Raman, and Padmanabhan, K. A., 1994 Tensile deformation-induced martensitic transformation in AISI 304LN austenitic stainless steel, Journal of Materials Science, Letters, 13, 389 - 392.

Garion, C., and Skoczeń, B., 2002 Modeling of strain-induced martensitic transformation for cryogenic applications, Journal of Applied Mechanics, 69, 755 – 762.

Hecker, S. S., Stout, M. G., Staudhammer, K. P., and Smith,J. L., 1982 Effect of strain state and strain rate on deformation-induced transformation in 304 stainless steel: Part I. Magnetic measurements and mechanical behavior, Metallurgical Transaction, 13A, 619 – 626.

Iwamoto, T., Tsuta, T., and Tomita, Y., 1998 Investigation on deformation mode dependence of strain-induced martensitic transformation in TRIP steels and modelling of transformation kinetics, International Journal Mechanical Science, 40, 173 – 182.

Kaleta, J., and Ziętek, G., 1998 Representation of cyclic properties of austenitic steels with plasticity-induced martensitic transformation (PIMT), Fatigue & Fracture of Engineering Materials & Structures, 21, 955 – 964.

Lebedev, A. A., and Kosarchuk, V. V., 2000 Influence of phase transformation on the mechanical properties of austenitic stainless steels, International Journal of Plasticity, 16, 749 – 767.

Levitas, V., 1998 Thermomechanical theory martrnsitic phase transformations in inelastic materials, 35, 889 – 940.

Levitas, V., Idesman, A., and Olson, G. B., 1999 Continuum modeling strain-induced martensitic transformation at shear-band intersection, Acta Mater., 47, 219 – 233.

Ludwigson, D. C., and Berger, J. A., 1969 Plastic behaviour of metastable austenitic stainless steels, Journal of the Iron and Steel Institute, 207,63 – 69.

Mahnken, R., Schneidt, A., and Antretter, T., 2009 Macro modeling and homogenization for transformation induced plasticity of a low-alloy steel, International Journal of Plasticity, 25, 183 – 204.

Maxwell, P. C., Goldberg, A., and Shyne,J. C., 1974 Stress-assisted and strain-induced martensite in Fe-Ni-C alloy, Metallurgical Transaction, 5, 1305 – 1318.

Mróz, Z., and Ziętek, G., 2007 Modeling of cyclic hardening of metals coupled with martensitic transformation, Arch. Mech., 59, 3 – 20.

Mughrabi, H., and Christ, H-J., 1997 Cyclic deformation and fatigue of selected ferritic and austenitic steels: specific aspects, The Iron and Steel Institute of Japan (ISIJ International). 37, 1145 – 1169.

Narutani, T., 1989 Effect of deformation-induced martensitic transformation on the plastic behavior of metastable austenitic stainless steel, Materials Transaction, JIM, 30, 33 – 45.

Olson, G. B., and Azrin, M., 1978 Transformation behavior of TRIP steels, Materials Transaction A, 9A, 713 – 721.

Olson, G. B., and Cohen, M., 1975 Kinetics of strain-induced martensitic nucleation, Materials Transaction A, 6A, 791 – 795.

Olson, G. B., and Cohen, M., 1982 Stress-assisted isothermal martensitic transformation: application to TRIP steels, Materials Transaction A, 13A, 1907 – 1913.

Onyuna, M. O., 2003 Deformation behaviour and martensitic transformations in metastable austenitic steels and low alloyed multiphase steels, Dissertation, Freiberg University of Mining and Technology.

Perdahcioğlu, E. S., Geijselaers, H. J.M., and Huétink, J., 2008 Influence of stress state and strain path on deformation induced martensitic transformations, Materials Science & Engineering A, 481-482, 727 – 731.

Stringfellow, R. G., Parks, D. M., and Olson, G. B., 1992 A constitutive model for transformation plasticity accompanying strain-induced martensitic transformation in metastable austenitic steels, Acta metall. mater. 40, 1703-1716.

Talonen, J., 2007 Effect of strain-induced α'-martensite transformation on mechanical properties of metastable austenitic stainless steels, Dissertation, Helsinki University of Technology.
Tamura, I., 1982 Deformation-induced martensitic transformation and transformation-induced plasticity in steels, Metal Science, 16, 245 – 253.
Tjong, S. C., and Ho, N. J., 1988 Transmission electron microscopy observations of strain-induced martensitic formation in fatigued Fe-21Mn-2.5Al Alloy, Materials Science & Engineering A, 102, 125 – 130.
Tomita, Y., and Iwamoto, T., 2001 Computational prediction of deformation behavior of TRIP steels under cyclic loading, International Journal Mechanical Science, 43, 2017 – 2034.
Tsuchida, N., and Tomota, Y., 2000 A micromechnic modeling for transformation induced plasticity, Materials Science & Engineering, A285, 345 – 352.

Appendix

The multipliers $\dot{\lambda}_1$ i $\dot{\lambda}_2$ specifying yield and transformation strain rate can be derived from the consistency conditions imposed on yield and transformation conditions, thus

$$dF_p/dt = 0 \text{ and } dF_{tr}/dt = 0, \tag{59}$$

and we have there from

$$\begin{aligned}
&\frac{\partial F_p}{\partial \sigma_{ij}}\dot{\sigma}_{ij} - \frac{\partial F_p}{\partial \sigma_{ij}}\dot{X}_{ij} - \frac{\partial F_p}{\partial \sigma_{kl}}\frac{\partial f_{kl}}{\partial Y_{ij}}\dot{Y}_{ij} + \frac{\partial F_p}{\partial \xi}\dot{\xi} = \\
&= \frac{\partial F_p}{\partial \sigma_{ij}}\dot{\sigma}_{ij} - \frac{\partial F_p}{\partial \sigma_{ij}}\left(C_1\frac{\partial F_p}{\partial \sigma_{ij}}\dot{\lambda}_1 - C_1 C X_{ij}\dot{\lambda}_1 - \dot{\lambda}_2 C_1 \frac{\partial F_{tr}}{\partial X_{ij}}\right) - \frac{\partial F_p}{\partial \sigma_{kl}}\frac{\partial f_{kl}}{\partial Y_{ij}}\left(C_2\frac{\partial F_p}{\partial \sigma_{mn}}\dot{\lambda}_1\frac{\partial f_{mn}}{\partial Y_{ij}} + \dot{\lambda}_2 C_2\frac{\partial F_{tr}}{\partial X_{ij}}\right) - \frac{\partial F_p}{\partial \sigma_{ij}} f_{ij}\frac{da}{d\xi}\dot{\lambda}_2\frac{dR_{tr}}{d\Sigma} = \\
&= \frac{\partial F_p}{\partial \sigma_{ij}}\dot{\sigma}_{ij} - \dot{\lambda}_1\left(\frac{3}{2}C_1 - C_1 C X_{ij}\frac{\partial F_p}{\partial \sigma_{ij}} + C_2\frac{\partial F_p}{\partial \sigma_{kl}}\frac{\partial f_{kl}}{\partial Y_{ij}}\frac{\partial F_p}{\partial \sigma_{mn}}\frac{\partial f_{mn}}{\partial Y_{ij}}\right) - \dot{\lambda}_2\left(C_2\frac{\partial F_p}{\partial \sigma_{kl}}\frac{\partial f_{kl}}{\partial Y_{ij}}\frac{\partial F_{tr}}{\partial X_{ij}} - C_1\frac{\partial F_p}{\partial \sigma_{ij}}\frac{\partial F_{tr}}{\partial X_{ij}} + \frac{\partial F_p}{\partial \sigma_{ij}} f_{ij}\frac{da}{d\xi}\frac{dR_{tr}}{d\Sigma}\right)
\end{aligned} \tag{60}$$

$$\begin{aligned}
&\frac{\partial F_{tr}}{\partial X_{ij}}\dot{X}_{ij} + \frac{\partial F_{tr}}{\partial Y_{ij}}\dot{Y}_{ij} + \frac{\partial F_{tr}}{\partial \Sigma}\dot{\Sigma} = \\
&= \frac{\partial F_{tr}}{\partial X_{ij}}\left(C_1\frac{\partial F_p}{\partial \sigma_{ij}}\dot{\lambda}_1 - C_1 C X_{ij}\dot{\lambda}_1 - \dot{\lambda}_2 C_1\frac{\partial F_{tr}}{\partial X_{ij}}\right) - \frac{\partial F_{tr}}{\partial X_{ij}}\left(C_2\frac{\partial F_p}{\partial \sigma_{kl}}\dot{\lambda}_1\frac{\partial f_{kl}}{\partial Y_{ij}} + \dot{\lambda}_2 C_2\frac{\partial F_{tr}}{\partial X_{ij}}\right) + \left(\frac{\partial F_{tr}}{\partial \Sigma}\right)^2\frac{d^2\varphi}{d\xi^2}\dot{\lambda}_2 = \\
&= \dot{\lambda}_1\left(C_1\frac{\partial F_p}{\partial \sigma_{ij}}\frac{\partial F_{tr}}{\partial X_{ij}} - C_1 C X_{ij} - C_2\frac{\partial F_p}{\partial \sigma_{kl}}\frac{\partial f_{kl}}{\partial Y_{ij}}\frac{\partial F_{tr}}{\partial Y_{ij}}\right) - \dot{\lambda}_2\left(3 - \left(\frac{\partial F_{tr}}{\partial \Sigma}\right)^2\frac{d^2\varphi}{d\xi^2}\right)
\end{aligned} \tag{61}$$

The multipliers $\dot{\lambda}_1$ and $\dot{\lambda}_2$ can be obtained as the solution of the system of two linear equations

$$A_{11}\dot{\lambda}_1 + A_{12}\dot{\lambda}_2 = \frac{\partial F_p}{\partial \sigma_{ij}}\dot{\sigma}_{ij} \quad \text{and} \quad A_{21}\dot{\lambda}_1 + A_{22}\dot{\lambda}_2 = 0 \tag{62}$$

where

$$A_{11} = \left(\frac{3}{2}C_1 - C_1 C X_{ij}\frac{\partial F_p}{\partial \sigma_{ij}} + C_2\frac{\partial F_p}{\partial \sigma_{kl}}\frac{\partial f_{kl}}{\partial Y_{ij}}\frac{\partial F_p}{\partial \sigma_{mn}}\frac{\partial f_{mn}}{\partial Y_{ij}}\right), \tag{63}$$

$$A_{12} = \left(C_2\frac{\partial F_p}{\partial \sigma_{kl}}\frac{\partial f_{kl}}{\partial Y_{ij}}\frac{\partial F_{tr}}{\partial X_{ij}} - C_1\frac{\partial F_p}{\partial \sigma_{ij}}\frac{\partial F_{tr}}{\partial X_{ij}} + \frac{\partial F_p}{\partial \sigma_{ij}} f_{ij}\frac{da}{d\xi}\frac{dR_{tr}}{d\Sigma}\right), \tag{64}$$

$$A_{21} = \left(C_1\frac{\partial F_p}{\partial \sigma_{ij}}\frac{\partial F_{tr}}{\partial X_{ij}} - C_1 C X_{ij} - C_2\frac{\partial F_p}{\partial \sigma_{kl}}\frac{\partial f_{kl}}{\partial Y_{ij}}\frac{\partial F_{tr}}{\partial Y_{ij}}\right), \tag{65}$$

$$A_{22} = \left(3 - \left(\frac{\partial F_{tr}}{\partial \Sigma}\right)^2\frac{d^2\varphi}{d\xi^2}\right). \tag{66}$$

Solution of the system of equations (62) provides the multipliers $\dot{\lambda}_1$ and $\dot{\lambda}_2$, thus

$$\dot{\lambda}_1 = \frac{A_{22}}{A_{11}A_{22} - A_{21}A_{12}}\frac{\partial F_p}{\partial \sigma_{ij}}\dot{\sigma}_{ij}, \qquad \dot{\lambda}_2 = \frac{A_{21}}{A_{21}A_{12} - A_{11}A_{22}}\frac{\partial F_p}{\partial \sigma_{ij}}\dot{\sigma}_{ij}. \tag{67}$$